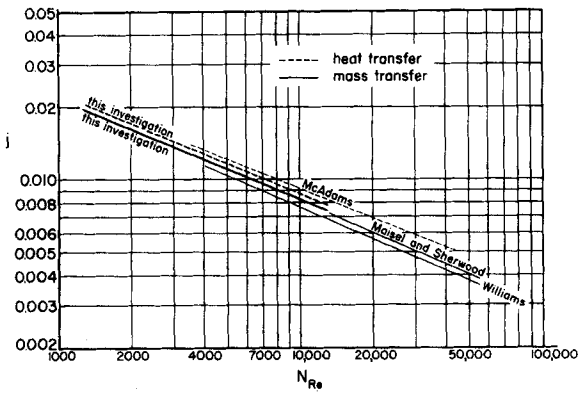

Fig. 4. Comparison of j-factor for single spheres resulting from this study with other available data.

t_d = dry-bulb temperature, °F.
t_s = surface temperature, °F.
t_w = wet-bulb temperature, °F.
μ = viscosity, lb./hr. ft.
ρ = density, lb./cu. ft.

LITERATURE CITED

1. Baumeister, E. B., and C. O. Bennett, *A.I.Ch.E. Journal*, **4**, 69 (1958).
2. Chilton, T. H., and A. P. Colburn, *Ind. Eng. Chem.*, **26**, 1183 (1934).
3. Gamson, B. W., George Thodos, and O. A. Hougen, *Trans. Am. Inst. Chem. Engrs.*, **39**, 1 (1943).
4. Gilliland, E. R., and T. K. Sherwood, *Ind. Eng. Chem.*, **26**, 516 (1934).
5. Glaser, M. B., and George Thodos, *A.I.Ch.E. Journal*, **4**, 63 (1958).
6. Lee, C. Y., and C. R. Wilke, *Ind. Eng. Chem.*, **47**, 1253 (1955).
7. Lynch, E. J., and C. R. Wilke, University of California Radiation Laboratory, *UCRL-8601* (January 14, 1959).
8. Maisel, D. S., and T. K. Sherwood, *Chem. Eng. Progr.*, **46**, 131 (1950).
9. McAdams, W. H., "Heat Transmission," 2 ed., p. 236, McGraw-Hill, New York (1942).
10. Williams, G. C., Sc. D. thesis, Mass. Inst. Technol., Cambridge (1942).

Manuscript received October 26, 1959; revision received April 7, 1960; paper accepted April 8, 1960.

Size Distribution of Droplets from Centrifugal Spray Nozzles

PAUL A. NELSON and WILLIAM F. STEVENS

Northwestern Technological Institute, Evanston, Illinois

Methods for expressing, measuring, and correlating drop-size distribution data for centrifugal spray nozzles are discussed.

A method for collecting spray droplets in liquid nitrogen is described which is rapid and efficient for most sprayed liquids which freeze above —20°C. Comprehensive correlations for drop-size distributions are reported based on 114 runs performed with the liquid nitogen method.

Studies of the kinetics of evaporation or combustion of droplets issuing from a spray nozzle require data on the size distribution of the droplets. Unfortunately these data are not easily obtained because the droplets are very minute and difficult to sample; also it is difficult to express and correlate drop-size data because the drops issuing from a spray nozzle are nonuniform in size.

The purpose of this paper is to report on methods of measuring, expressing and correlating drop-size data which the writers found to be successful in a recent study of grooved-core centrifugal spray nozzles.

DISTRIBUTION FUNCTIONS

A theoretical distribution function for expressing drop-size distributions has not been derived as yet. The best that can be done with experimental data is to express the distribution graphically or to specify a distribution function and the values of the parameters in the distribution equation which will most closely represent the data.

Several of the distribution functions which have been proposed are based on the normal distribution, and only this type will be discussed:

$$f_v(y) = \frac{dv}{Vdy} = \frac{1}{s\sqrt{2\pi}} e^{-\frac{(y-\bar{y})^2}{2s^2}} \qquad (1)$$

Equation (1) is the normal distribution equation expressed in terms of the volume of droplets.

The size characteristic is a function of the drop diameter. However if the drop diameter itself is chosen as the size characteristic, experimental data will not fit the distribution. Three size characteristics which have been successfully used are the log of the drop diameter (*6*), the upper limit characteristic (*10*), and the square-root of the drop diameter (*15*).

The log-normal distribution and the square-root normal distribution have two parameters, a mean and a standard deviation, which can be adjusted to fit a particular set of data. The upper-limit distribution has a third parameter, the maximum stable drop size, which permits more flexibility in fitting experimental data.

From a theoretical standpoint the upper-limit distribution has another advantage over the log-normal distribution and the square-root normal distribution in that it places reasonable limits on the minimum and maximum drop size. However despite the fact that the extreme ends of the distribu-

Paul A. Nelson is with the Chemical Engineering Division, Argonne National Laboratory, Lemont, Illinois.

tion curve derived from the square-root normal function lead to physical absurdities, the square-root normal distribution has been found to be useful in expressing data from centrifugal pressure nozzles within two standard deviations of the square-root mean. In Figure 1 the three distributions are compared. The upper-limit function and the square-root-normal function approximate a typical experimental drop-size distribution for a centrifugal nozzle. However the log-normal distribution deviates quite far from the other functions which represent actual data more closely.

The square-root-normal distribution was found to be useful in expressing the data obtained in this investigation, in addition to the many times it has been used previously by other investigators (*1, 2, 8, 15*). Therefore a method was sought and developed for determining the Sauter mean diameter from the volume median diameter (the square of the square-root-normal mean) and the square-root-normal standard deviation. The Sauter mean diameter is of interest because the surface-to-volume ratio can be calculated directly from the Sauter mean by the following relationship:

$$s_v = \frac{\int_{x_o}^{x_m} \pi x^2 f_n(x)\,dx}{\int_{x_o}^{x_m} \frac{\pi}{6} x^3 f_n(x)\,dx} = \frac{6}{\bar{x}_{vs}} \qquad (2)$$

The desired relationship was derived from the square-root-normal distribution function and Equation (2):

$$\bar{x}_{vs} = \frac{\tilde{x}}{\int_{x_o}^{x_m} \frac{1}{\left[\frac{sz}{\sqrt{\tilde{x}}} + 1\right]^2} \frac{1}{\sqrt{2\pi}} e^{-\frac{z^2}{2}}\,dz} \qquad (3)$$

The integral was evaluated graphically for several values of $s/\sqrt{\tilde{x}}$ as described in detail by Nelson (*11*). The results are plotted in Figure 2. From this graph the Sauter mean diameter can be obtained from the volume median diameter and the square-root-normal standard deviation.

EXPERIMENTAL PROCEDURE AND EQUIPMENT

To obtain the experimental data of this investigation spray droplets were frozen by a technique employing liquid nitrogen. Others have used various frozen-drop methods with liquids freezing both above (*4, 5*) and below (*1, 7, 16*) room temperature. The first one to use liquid nitrogen as a freezing medium for sprays was A. P. R. Choudhury at Northwestern University (*1*) who found that the frozen particles dried almost immediately when the liquid nitrogen was decanted, permitting dry screening in a cold room. However it was not possible to collect sprayed liquids with densities less than 1.2.

In order to remove the density restriction special equipment was designed and built for freezing the droplets. A diagram of the spray collector is shown in Figure 3. The spray collector was an insulated chamber having an inside diameter of approximately 20 in. Liquid nitrogen sprayed from perforated copper tubing near the top of the chamber at a rate of 3 to 5 liters/min. and flowed down the inside surface of the collector. The surface of the collector within the spray pattern of a centrifugal nozzle was completely covered with a flowing film of liquid nitrogen. Droplets sprayed into the chamber were at least partially frozen by the cold atmosphere evolved from the evaporating nitrogen and completely frozen and carried out of the chamber by the liquid nitrogen running down the walls of the collector. The droplets were screened from the liquid nitrogen flowing from the collector by nine sieves which were 8 in. in diameter by 1 in. high. During the test gaseous nitrogen at room temperature was admitted above the nozzle at a rate slow enough not to affect atomization, in order to push back the cold atmosphere from the area around the nozzle. Temperature measurements indicated that the properties of the gas in the immediate area of the spray nozzle were those of the gas admitted above the nozzle (11). As soon as the collector had been cooled to the temperature of boiling liquid nitrogen, the solenoid feed valve was operated and the nozzle began to spray. The first and last part of the spray was prevented from going into the collector by a drawer which slid on tracks just beneath the nozzzle. The cut-off drawer operated a switch which actuated an electric timer, thus permitting calculation of the amounts sprayed from knowledge of the flow rate.

Some of the finest frozen droplets were washed through all of the sieves into the container below by the flow of liquid nitrogen. This material was recovered by filtering the liquid nitrogen which had been collected through a tared filter paper. The filter paper and contents were later weighed with the bottom pan.

After the spray had been turned off and the inside of the collector thoroughly rinsed with liquid nitrogen, the sieves were transferred to an insulated container with enough liquid nitrogen to keep the droplets frozen during a half-hour shaking period. The equipment employed for shaking was rebuilt to accommodate the insulated sieve container.

At the end of the shaking period the sieve container was removed to a cold box shown in Figure 4. The 2-ft. cubical cold chamber was cooled by cold air circulated by a fan through a dry ice chamber. The sieves were weighed in this cold box on a triple beam balance which was supported on top of the cold chamber by a sheet of clear plastic.

The main features of this method are the following:

1. Essentially all of the spray is collected, thus minimizing sampling errors. The average recovery of material sprayed was 91% for the 111 runs for which data were available.
2. The only restriction on the material sprayed is that its melting point must be high enough to permit screening and weighing. Runs were made with materials melting as low as −20°C. with ease.
3. Shattering of the droplets as they strike the collecting medium is minimized because the particles are partially frozen in the cold atmosphere inside the collecting chamber before they strike the liquid nitrogen surface.
4. The screening technique is limited to sprays with a volume median drop diameter greater than 38μ, although finer droplets could be photographed and measured.
5. The method is relatively rapid and inexpensive. It was possible for a single operator to make three to four runs per day.

TABLE 1. NOZZLE CHARACTERISTICS
Spraying System Co., Type SL Spray Drying Nozzle

No.	Orifice Diameter, in.	No.	Core Flow area, sq. in.	Spray angle	Capacity, gal./hr. of water at 1000 lb./sq. in.
80	0.0135	10	3.6×10^{-4}	56°	4.0
		16	7.7	52	5.1
74	0.0225	20	12.4	62	9.9
67	0.032	20	12.4	74	14.1
		17	15.4	70	16.7
		21	28	64	24.5
58	0.042	17	15.4	81	22.2
54	0.055	17	15.4	91	29.6
		21	28	85	45.3
		27	48	73	70.2
46	0.081	27	48	84	112

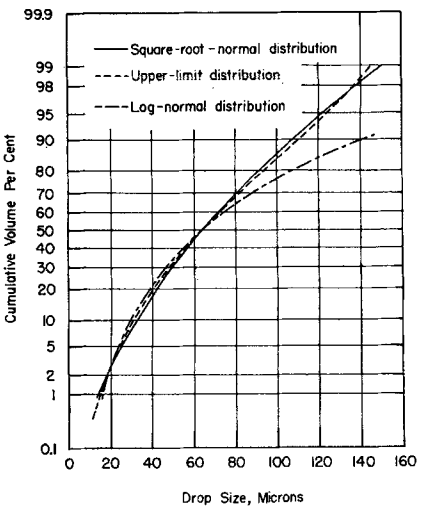

Fig. 1. Comparison of square-root-normal, upper-limit, and log-normal distributions.

CHOICE OF NOZZLES AND MATERIALS INVESTIGATED

A wide range of nozzle sizes, spraying pressures, and liquid properties were covered in the 114 runs made by this technique. The nozzle chosen is of the grooved-core type with interchangeable orifice inserts.

The manufacturer's data (*14*) for the orifice inserts and cores employed in this study is shown in Table 1.

The type of nozzle chosen for this study has been employed by other investigators who showed that it has many good properties. McIrvine (*9*) showed that for the viscosity range 1 to 10 centipoises, viscosity does not appreciably affect nozzle capacity, cone angle, or air core diameter. Darnell (*2*) showed that the capacity is proportional to the square root of the pressure and that the diameter of the air core is independent of pressure. Thus it was possible to vary the axial velocity without changing the cone angle or the air core diameter.

The axial velocity was varied by changing the pressure on the feed tank between pressure limits of 100 and 1,500 lb./sq. in. gauge. The pressure was measurable to within 1% by accurate gauges.

On the basis of their physical properties the following seven liquids were chosen for spraying: cyclohexane, *n*-octyl alcohol, carbon tetrachloride, water, nitrobenzene, aniline, and 1,1,2, 2-tetrabromoethane. The melting points of these materials vary from −22.6° to 6.5°C. The viscosity of these liquids varies tenfold, the density varies fourfold, and the surface tension threefold. The properties of the materials sprayed covered ranges which include almost all materials presently being sprayed with pressure nozzles with the exception of fuel oils having viscosities greater than 10 centipoises.

EXPERIMENTAL RESULTS

The most important evidence of the method's validity are microphotographs which show that the screened particles are round and fairly uniform in size. One of the pictures, taken by the method of Remus (*12*), of particles screened through the 74-μ sieve and collected on the 62-μ sieve is shown in Figure 5. On a weight basis there is only a small percentage of undersized particles. The fuzzy appearance of the particles is due to water vapor that was observed to condense before the picture was taken. No broken particles or agglomerations of smaller particles were evident in any of the microphotographs of screened particles.

For the 111 runs for which recovery data were available the average recovery was 91.1% of the material sprayed. One of the most common causes of low recovery was loss of material from between the sieves during shaking due to inadequate clamping of the sieves. Complete experimental and calculated data for the 114 successful runs have been tabulated and are on file with the American Documentation Institute.*

For all of the materials and nozzle combinations investigated the data appeared to fit the square-root-normal distribution function. This was determined by plotting the cumulative mass

* Tabular material has been deposited as document 6530 with the American Documentation Institute, Photoduplication Service, Library of Congress, Washingon 25, D. C., and may be obtained for $2.50 for photoprints or $1.75 for 35-mm. microfilm.

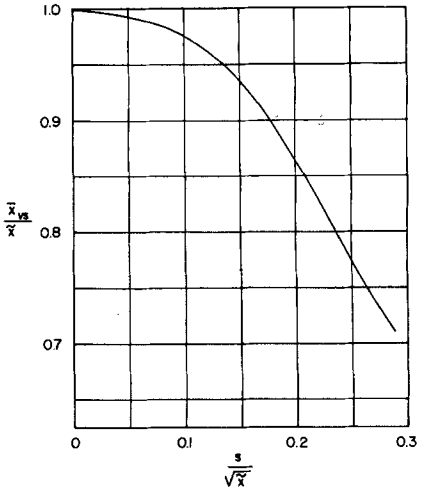

Fig. 2. Relationship between the Sauter mean diameter and the volume median diameter and square-root-normal standard deviation.

vs. the square root of the sieve size on normal probability paper as shown in Figure 6. In all cases a straight line was obtained within the accuracy of the data. The volume median was obtained by squaring the value of the square-root of the drop diameter at 50 cum. wt. %. The square-root-normal standard deviation was determined from the graph by subtracting the square-root-normal mean from the square root of the drop size at one standard deviation above the mean which corresponds to 84.13 cum. wt. %.

It is known that sieves finer than 200 mesh are not very accurate, but in this investigation it was necessary to use sieves ranging down to 400 mesh. However it may be observed from

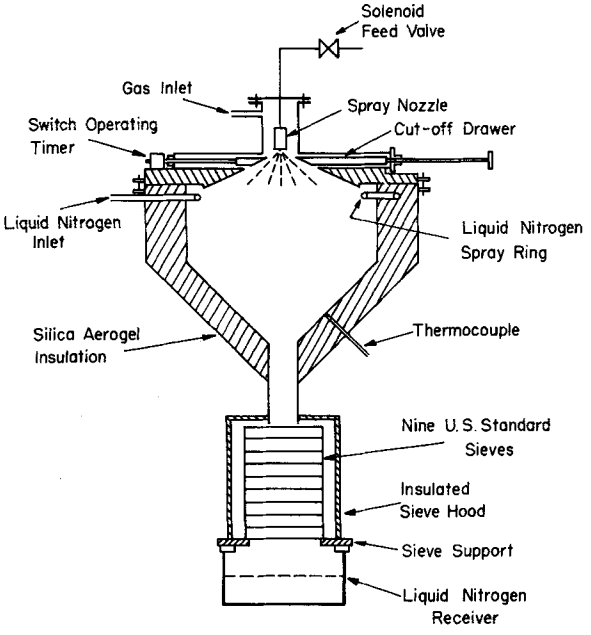

Fig. 3. Diagram of spray collector.

Figure 6 that the inaccuracies of the sieves were partially compensated for by drawing a straight line through the points. The points for a given sieve are either consistently above or consistently below the lines of best fit. For instance the points corresponding to the 230-mesh sieve were always above the curve of best fit, and the points corresponding to the 325-mesh sieve were always below. It was assumed that the deviations of the data from the lines of best fit were due mainly to inaccuracies in the sieves.

Only a few duplicate runs were made during the investigation, so little information was gained from these runs concerning the reproducibility of the data. However graphical comparisons of runs made at varying pressures with the same nozzle and material indicate that, under these conditions, the standard deviation for the volume median diameter and the square-root-normal standard deviation were approximately 3 and 8% respectively.

CORRELATION OF THE DROP-SIZE DATA

The data obtained in this investigation were correlated by dimensional analysis because the problem of liquid breakup from a centrifugal pressure nozzle is very difficult to approach theoretically. Fluid flow through centrifugal nozzles has not yet been adequately treated, but even if the velocity and pressure distributions in the nozzle were known, it would still be difficult to relate them to the drop-size distribution obtained.

The basic assumption in the correlation of the data is that the flow characteristics of the liquid flowing through the orifice can be defined by variables which do not include nozzle dimensions related to a particular design; that is all flow characteristics peculiar to a nozzle design are damped out by the high turbulence in the flow through the orifice. This assumption was used to correlate the air core diameter data of Darnell (2) and McIrvine (9) in order to indicate the feasibility of this approach for the problem of correlating the drop-size data.

The diameter of the air core formed at the axis of the nozzle is affected by the variables shown in the following relationship:

$$D_c = f(V_a, V_t, D_o, \mu, \rho, e) \qquad (4)$$

The geometry and dimensions peculiar to each particular centrifugal nozzle and the pressure drop through the nozzle have not been neglected because these characteristics will be reflected in the average tangential velocity, the average axial velocity, the roughness, and the orifice diameter.

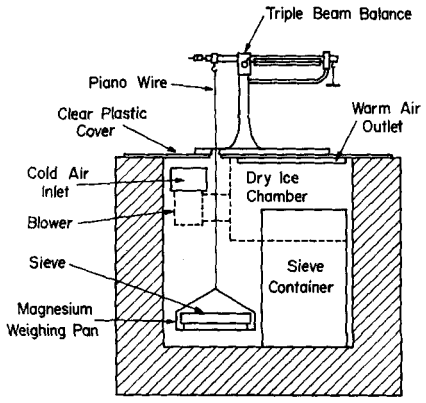

Fig. 4. Diagram of cold chamber for weighing sieves.

The effects of air resistance inside the core, surface tension, and wettability of the fluid for the nozzle were neglected. When combined by dimensional analysis these variables lead to the dimensionless groups shown in the following relationship:

$$\frac{D_c}{D_o} = f\left[\frac{D_o V_a \rho}{\mu}, \frac{V_t}{V_a}, \frac{e}{D_o}\right] \qquad (5)$$

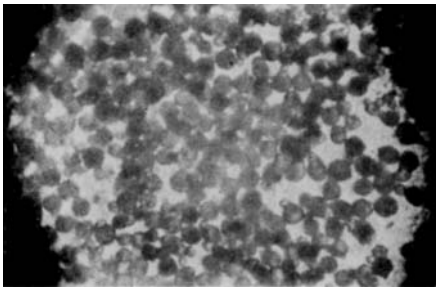

Fig. 5. Microscopic view of screened particles.

The velocity ratio V_t/V_a has been obtained through measurement of the mass of spray collected in concentric rings placed beneath the nozzle (2, 13, 15). However at pressures above 200 lb./sq. in. gauge it is doubtful that such data would correlate with the flow characteristics in the nozzle because of air turbulence which disperses the droplets. It is believed that a better index of the true V_t/V_a ratio is the maximum cone angle which can be readily measured photographically or with calipers; that is

$$\theta_m = f\left(\frac{V_t}{V_a}\right) \qquad (6)$$

The first group in Equation (5) appears to have little effect on the air core to orifice ratio as indicated by experimental data. For instance Darnell (2) showed that beyond pressures where the cone angle is independent of pressure change the air core diameter was also unaffected by pressure change. Also the data of McIrvine (9) indicated only a slight decrease in the cone angle with increasing viscosity. Therefore the Reynolds number was neglected. In addition the roughness group e/D_o was neglected in order to simplify the relationship.

Since the other dimensionless groups were eliminated, D_c/D_o was plotted against θ_m (assumed to be a function of V_t/V_a) as shown in Figure 7 for the data of Darnell (2) and McIrvine (9). The boundary conditions at air core to orifice diameter ratios of zero and one were helpful in determining the general shape of the curve. Each point was calculated by averaging the data for D_c/D_o at six different pressures, 100, 400, 700, 1,000, 1,300, and 1,600 lb./sq. in. gauge except for the smallest nozzles of 0.0135- and 0.020-in. diameter for which the D_c/D_o ratio was averaged for the pressures 700, 1,000, 1,300, and 1,600 lb./sq. in. gauge and for 400, 700, 1,000, 1,300, and 1,600 lb./sq. in. gauge respectively (11). When one considers the difficulty in measuring the data and the fact that the roughness group was neglected, the correlation is satisfactory and tends to corroborate the assumption that the characteristics of the flow through the orifice are determined by the variables in Equation (4).

It should be noted that this result does not disagree with the theoretical work of those who relate the air core diameter to nozzle dimensions only [Doumas and Laster (3)], for the cone angle is itself a function of the nozzle dimensions only, over a wide range of liquid properties as demonstrated by McIrvine (9).

It was assumed that the same type of approach would be successful for correlating the drop-size distribution data obtained in this investigation by the frozen-drop technique which was

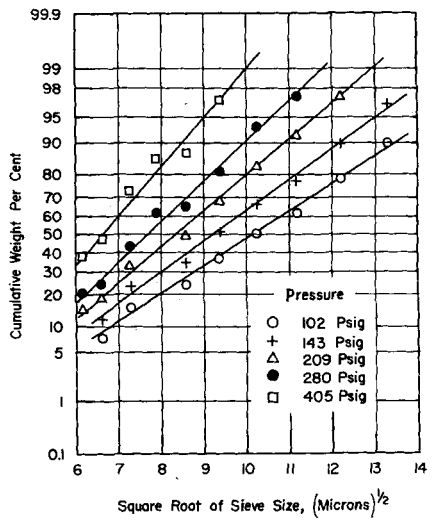

Fig. 6. Drop-size data illustrating the good fit to the square-root-normal distribution.

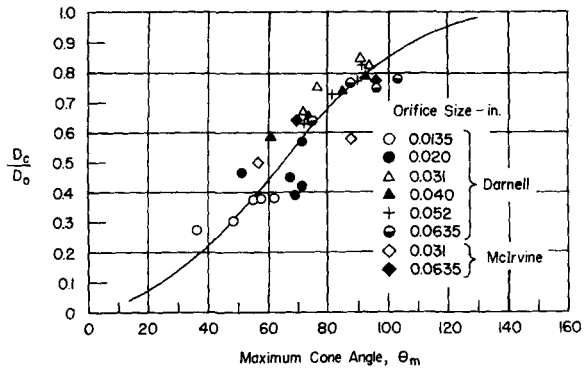

Fig. 7. Ratio of air core to orifice diameter vs. the maximum cone angle.

previously described. In this case a separate correlation must be derived for each parameter in the distribution function describing the data. Also another variable must be considered, the surface tension of the liquid sprayed, because the surface involved in drop formation is much greater than that involved in formation of the air core. For a distribution function expressed by two parameters, such as a mean or median and a standard deviation, two independent relationships result from this approach:

$$\bar{x} = f(V_a, V_t, D_o, \mu, \rho, \sigma, e) \quad (7)$$

$$s = g(V_a, V_t, D_o, \mu, \rho, \sigma, e) \quad (8)$$

By dimensional analysis the number of independent variables can be reduced from seven to four:

$$\frac{\bar{x}}{D_o} = \phi\left[\frac{D_o V_a \rho}{\mu}, \frac{V_a^2 D_o \rho}{\sigma}, \frac{V_t}{V_a}, \frac{e}{D_o}\right] \quad (9)$$

$$\frac{s}{D_o^t} = \psi\left[\frac{D_o V_a \rho}{\mu}, \frac{V_a^2 D_o \rho}{\sigma}, \frac{V_t}{V_a}, \frac{e}{D_o}\right] \quad (10)$$

where t has a value such that s/D_o^t is dimensionless. These equations were simplified by neglecting the roughness factor group e/D_o. By reasoning in a manner similar to that leading up to Equation (6), the group V_t/V_a was assumed to be a function of $[V_t/V_a]_*$ only, which is defined by

$$\left(\frac{V_t}{V_a}\right)_* = \tan\frac{\theta_m}{2} \quad (11)$$

By making these simplifications and considering the square-root-normal distribution one obtains

$$\frac{\tilde{x}}{D_o} = \phi\left[N_{Re}, N_{We}, \left(\frac{V_t}{V_a}\right)_*\right] \quad (12)$$

In this investigation the manufacturer's data for the maximum cone angle, listed in Table 1, were employed to calculate $(V_t/V_a)_*$. The manufacturer's data also were used for the orifice diameter. The axial velocity was calculated from measured flow numbers for each liquid and nozzle combination according to the following equation:

$$V_a = \frac{F_n\sqrt{p}}{\frac{\pi D_o^2}{4}\left[1 - \left(\frac{D_c}{D_o}\right)^2\right]} \quad (13)$$

The D_c/D_o ratio was calculated from curves through Darnell's data (2). However it could have been obtained from Figure 7 with about the same results.

By trial-and-error plotting of the data it was shown that the volume median drop diameters obtained by spraying six organic liquids with eleven different nozzle orifice and core insert combinations over a pressure range of 100 to 1,500 lb./sq. in. gauge could be correlated according to the relationship of Equation (9). The results are shown in Figure 8. The equation of the curve of best fit is

$$Y = -0.0811Z^2 + 0.124Z - 0.186 \quad (14)$$

where

$$Y = \log_{10}\frac{\tilde{x}}{D_o}$$

$$Z = \log_{10}\left[N_{Re}\left(\frac{N_{We}}{N_{Re}}\right)^{0.55}\left(\frac{V_t}{V_a}\right)_*^{1.2}\right]$$

The average deviation of the experimental volume median diameter from this curve was 8.25% for a range of volume median diameters of from 39.6 to 162.5μ. The deviations did not appear to be related to the orifice diameter, the spray cone angle, the particular liquid sprayed, or the pressure drop through the nozzle. Each particular nozzle gave a curve which was slightly different from the curve for the entire data, but the difference could not be related to the nozzle properties of orifice diameter and spray cone angle. Consequently the deviations from the curve of Figure 8 appeared to be due to experimental error, slight irregularities in the nozzles, the neglecting of pertinent variables from the dimensional analysis, and the approximation made in plotting a four-dimensional relationship [Equation (12)] on a two-dimensional graph.

The data for the volume median drop diameter for water sprays did not agree with the data for the organic liquids. If plotted on Figure 8 the data for water would lie 30 to 50% above the curve of best fit for the organic liquids. There is a possibility that the water did not wet the nozzle wall and that this caused the difference. The data obtained in thirteen runs with water were plotted with the data obtained by Darnell (2) with the same

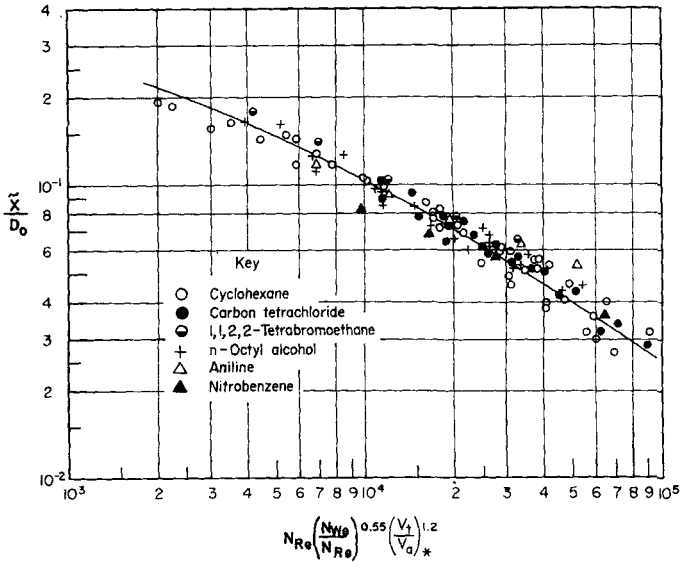

Fig. 8. Correlation of volume median diameter for liquids other than water.

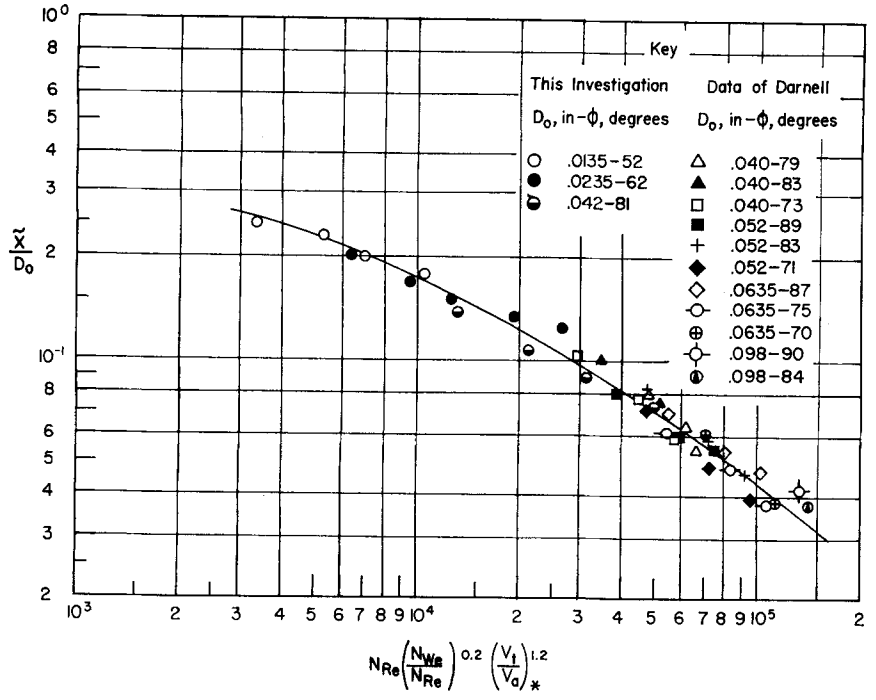

Fig. 9. Correlation of volume median diameter for water.

type of nozzle, as shown in Figure 9. Darnell's data were obtained by photographing droplets collected in an immiscible liquid at 10 in. below the nozzle.

The equation for the curve of best fit for the water data is similar to that obtained for the organic liquids:

$$Y = -0.144Z^2 + 0.702Z - 1.260 \qquad (15)$$

where

$$Y = \log_{10}\frac{\tilde{x}}{D_o}$$

$$Z = \log_{10}\left[N_{Re}\left(\frac{N_{We}}{N_{Re}}\right)^{0.2}\left(\frac{V_t}{V_a}\right)^{1.2}_*\right]$$

The average deviation of the data from this equation is 6.7%.

Adopting the same simplifications as were utilized for obtaining Equation (12) from Equation (9) one obtains for the square-root-normal distribution from Equation (10)

$$\frac{s}{\sqrt{D_o}} = \psi\left[N_{Re}, N_{We}, \left(\frac{V_t}{V_a}\right)_*\right] \qquad (16)$$

By trial-and-error plotting of the data it was shown that all of the standard deviation data of this investigation (for both organic materials and water) fit one form of this equation. The results are shown in Figure 10 in which

$$\frac{s}{\sqrt{D_o}}N_{We}^{0.5}$$

was plotted against

$$\left(\frac{N_{We}}{N_{Re}}\right)N_{Re}^{0.5}$$

Within the accuracy of the data the effect of $(V_t/V_a)_*$ was negligible.

The equation for the curve of best fit is

$$Y = 0.150Z^2 - 0.359Z + 0.986 \qquad (17)$$

where

$$Y = \log_{10}\frac{s}{\sqrt{D_o}}N_{We}^{0.5}$$

$$Z = \log_{10}\left[\left(\frac{N_{We}}{N_{Re}}\right)(N_{Re})^{0.5}\right]$$

The average deviation of the data from this equation is 13.0% for a range of square-root-normal standard deviations of from 0.80 to 3.44$\mu^{1/2}$. It is apparent that the data points are not as well distributed about the curve of best fit as for the correlations of the median. For instance the points representing carbon tetrachloride lie above the curve, while those representing cyclohexane lie below the curve, with few exceptions. However it is very difficult to determine the standard deviation accurately. Slight discrimination against a size class of particles, say the smaller particles, by the sampling or measuring techniques will not greatly affect the general shape of the distribution curve or the value of the median, but it may have a drastic effect on the standard deviation.

It would have been possible to substitute the superficial average velocity for the calculated average velocity because V_a' is a function of variables which have already been considered: $V_a' = f(V_a, D_o, D_c)$. A rough analysis of the data has shown that they could have been correlated with dimensionless groups based on the superficial velocity with results as good as were obtained with the calculated average velocity (but with different correlation curves resulting).

EFFECT OF OTHER VARIABLES

It was assumed that the properties of the gas medium have little effect on atomization at injection pressures below 1,500 lb./sq. in. gauge. Most of the runs were conducted with nitrogen gas surrounding the nozzle but two runs were conducted at 1,200 lb./sq. in. injection pressure in which helium gas was admitted through the gas inlet above the nozzle. A comparison of these runs with a similar run made

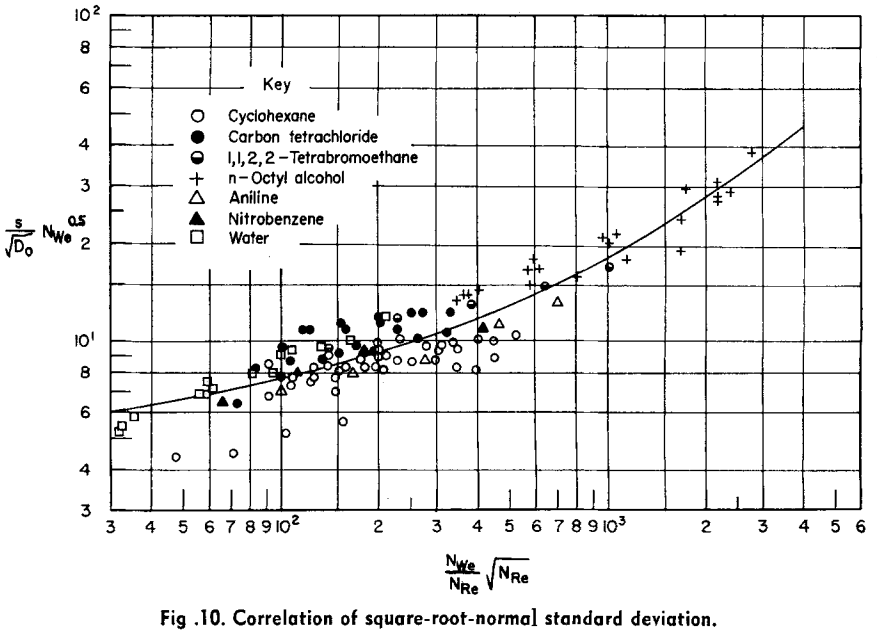

Fig .10. Correlation of square-root-normal standard deviation.

with a nitrogen atmosphere indicated that the properties of the atmosphere had no effect on atomization for centrifugal nozzles spraying at moderate pressures.

A little information was obtained during the investigation about the effect of nozzle roughness on atomization, but it was not extensive enough to include in the general correlations. For instance it was noted that corrosion of the nozzle parts which caused roughness resulted in larger mean drop sizes. A nozzle that was unintentionally polished with grinding compound produced a finer spray. Also use of a tungsten carbide orifice insert which appeared to be smoother than the standard steel insert resulted in a finer spray (*11*).

In conclusion the method of correlation utilized in this investigation appears to be valid, because satisfactory correlations were obtained for widely varying spraying conditions. The correlations obtained from the drop-size data for the particular design of grooved-core nozzles utilized in this investigation may be fairly accurate for other hollow-core nozzles. This is reasonable because the correlation variables are properties and dimensions of the spray itself as it issues from the nozzle, rather than characteristics of the spraying system (such as pressure drop or internal nozzle dimensions).

ACKNOWLEDGMENT

This work was sponsored by Project SQUID, which is supported by the Office of Naval Research, Department of the Navy, under contract N(onr)-1858(25) NR-098-038.

NOTATION

D_c = air core diameter
D_o = nozzle orifice diameter
e = orifice roughness factor, length dimensions
f = functional notation
$f_n(x)$ = dn/Ndx = frequency function, rate of change of the number of droplets with respect to the droplet diameter x, per unit number of droplets
$f_v(y)$ = dn/Vdy = frequency function, rate of change of the volume of droplets with respect to the size characteristic, y, per unit volume of droplets
F_n = flow number, ratio of volumetric flow rate to the square-root of the pressure drop through the nozzle (the flow number is usually a constant for a particular nozzle and a particular liquid)
n = number of droplets
N = total number of droplets in liquid sprayed
N_{Re} = Reynolds number, $D_o V_a \rho/\mu$
N_{We} = Weber number, $V_a^2 D_o \rho/\sigma$
r = radial distance from center of orifice
R_c = air core radius
R_o = orifice radius
s = standard deviation, and square-root-normal standard deviation
S_V = surface to volume ratio of a spray
t = a constant in Equation (10) which is adjusted so that s/D_o^t is dimensionless
v = volume of droplets
v_a = axial velocity at some radius, r, within the orifice of the nozzle
v_t = tangential velocity at some radius, r, within the orifice of the nozzle
V = total volume of droplets in liquid sprayed
V_a = mass-average axial velocity through the orifice,

$$\frac{\text{volumetric flow rate}}{\text{area of flow}} = \frac{\int_{R_c}^{R_o} 2v_a r\,dr}{(R_o^2 - R_c^2)}$$

V_a' = superficial mass-average axial velocity through the orifice,

$$\frac{\text{volumetric flow rate}}{\text{area of orifice}} = \frac{\int_{R_c}^{R_o} 2v_a r dr}{R_o^2}$$

V_t = mass-average tangential velocity through the orifice,

$$\frac{\int_{R_c}^{R_o} 2v_t r dr}{(R_o^2 - R_c^2)}$$

$\left(\frac{V_t}{V_a}\right)_* = \tan \theta_{m/2}$
x = droplet diameter
$\bar{x}$ = unspecified mean value of x
$\tilde{x}$ = volume median drop diameter, that drop diameter at which half of the volume of the spray is contained in drops having diameters smaller than $\tilde{x}$ and half of the volume of the spray is contained in drops having diameters larger than $\tilde{x}$
x_m = maximum stable drop diameter
x_o = minimum drop diameter
x_{vs} = Sauter mean diameter
$\underline{y}$ = size characteristic
$\bar{y}$ = mean value of y
y_o = ln x = size characteristic for log-normal distribution
y_s = $\sqrt{x}$ = size characteristic for square-root-normal distribution
y_u = ln $x/x_m - x$ = size characteristic in upper-limit distribution
z = $\sqrt{x} - \sqrt{\tilde{x}}/s_r$
Z = various groups of independent variables as defined in Equations (14), (15), and (17)

Greek Letters

θ_m = maximum cone angle determined by measuring with calipers directly on the spray or by measuring a photograph of the spray
ρ = density of liquid sprayed
σ = surface tension of liquid sprayed
μ = viscosity of liquid sprayed
ϕ = functional notation
ψ = functional notation

LITERATURE CITED

1. Choudhury, A. P. R., Ph.D. thesis, Northwestern Univ., Evanston, Illinois (1955).
2. Darnell, W. H., Ph.D. thesis, Univ. Wisc., Madison (1953).
3. Doumas, M., and R. Laster, *Chem. Eng. Progr.*, **49**, 518 (1953).
4. Joyce, J. R., *J. Inst. Fuels*, **22**, 150 (1949).
5. ———, *Tech. Report No. I.C.T. 17*, The Shell Petroleum Co., Ltd., Norman House, Strand, London (1950).
6. Kottler, F., *J. Franklin Inst.*, **250**, 339, 419 (1950).
7. Longwell, J. P., Doctoral dissertation, Mass. Inst. Technol., Cambridge (1943).
8. Marshall, W. R., Jr., *Chem. Eng. Progr. Monograph Ser. No. 2*, **50** (1954).
9. McIrvine, J. S., M.S. thesis, Univ. Wisc., Madison (1953).
10. Mugele, R. A., and H. D. Evans, *Ind. Eng. Chem.*, **43**, 1317 (1951).
11. Nelson, P. A., Ph.D. thesis, Northwestern Univ., Evanston, Illinois (1958).
12. Remus, G. A. P., M.S. thesis, Northwestern Univ., Evanston, Illinois (1954).
13. Rupe, J., "Third Symposium on Combustion and Flame and Explosion Phenomena," Williams and Wilkins Co. (1949).
14. Spraying Systems Co. Catalog No. 24, Bellwood, Illinois.
15. Tate, R. W., and W. R. Marshall, Jr., *Chem. Eng. Progr.*, **49**, 161, 226 (1953).
16. Taylor, E. H., and D. B. Harmon, Jr., *Ind. Eng. Chem.*, **46**, 1455 (1954).

Manuscript received April 13, 1959; revision received May 23, 1960; paper accepted May 23, 1960. Paper presented at A.I.Ch.E. Cincinnati meeting.